PFC/RR-91-8 DOE/PC-90350-2

DC CICC Retrofit Magnet Preliminary Design, Protection Analysis and Software Development

Quarterly Progress Report
Contract No. DE-FG22-90PC90350

J.H. Schultz, P.G. Marston and A.M. Dawson

December 1990
Issued April 1991

Plasma Fusion Center
Massachusetts Institute of Technologyy
Cambridge, Massachusetts 02139, USA

This work was supported by the U.S. Department of Energy, Pittsburgh Energy Technology Center, Pittsburgh, PA 15236, under Contract No. DE-FG22-90PC90350. Reproduction. translation, publication, use and disposal, in whole or part, by or for the United States Government is permitted.

Preliminary Analysis of the Proof-of-Concept Conductor Tests
On a CICC for Large-scale MHD Magnets

INTRODUCTION

The work reported herein is part of that necessary to analyse a retrofit MHD generator built using advanced DC cable-in-conduit conductor that was developed under DOE PETC contract DE-AC22-84PC70512 and which is now being further evaluated and studied analytically.

The work reported herein is the first step in the development of more sophisticated analytical software necessary to evaluate and predict the behavior of cable-in-conduit superconductors. This work and magnet design efforts are proceeding in parallel.

BACKGROUND

MIT has conducted a series of protection/quench experiments of two different topologies of candidate ICCS conductors for use in MHD magnets. The principal difference between them was that one had an insulating sleeve between the superconducting cable and its conduit, while the other, more conventional, conductor did not. The dimensions of the two conductors are described in Table 1.

Table I

Dimensions of Candidate Conductors

Dimension	Units	Sleeved	Unsleeved
No. Strands		27	27
Cable RRR		100?	100?
I_c	(kA)		
Strand Diameter	(mm)	0.76	0.76
Cu:SC		1.35	1.35
A_{strand}	(mm^2)	0.456	0.456
A_{noncu}	(mm^2)	0.194	0.194
A_{Cu}	(mm^2)	0.262	0.262
$A_{strands}$	(mm^2)	12.3	12.3
$A_{noncu,cable}$	(mm^2)	5.23	5.23
$A_{Cu,cable}$	(mm^2)	7.07	7.07
A_{He}	(mm^2)	6.6	7.5
f_{he}		0.33	0.38
P_{cable}	(mm)	12.25	12.25
$P_{cable+conduit}$	(mm)		28.01923656
$t_{sleeve\ (12\ mils)}$	(mm)	0.305	0
Conduit ID	(mm)	5.02	5.02
Conduit OD	(mm)	6.73	6.73
$t_{conduit}$	(mm)	0.855	0.855
$A_{cable\ space}$	(mm^2)	19.79	19.79

The manufacturer of the superconductor was Supercon. Their data on the superconductor critical properties are shown in Table II.

Table II

Manufacturer's Data on Superconductor Properties

vs. Measured and Calculated Properties

Flux Density	T_c	I_c	$I_{quench, measured}$	$T_{c,calc}$	$I_{c,calc}$
(T)	(K)	(A)	(A)	(K)	(A)
0	9.5		100	9.30	20,936.87
2	8.2			8.55	16,828.85
4	7.25			7.74	12,814.69
5		9990	6910	7.32	10,851.30
6	6.4	8100	5630	6.88	8,923.35
7		6480	4250	6.42	7,037.34
8	5.6			5.93	5,201.97
10	4.8			4.86	1,737.00

ANALYSIS

The analysis is proceeding along two parallel paths. One includes the development of detailed software to understand the complex electromagnetic and thermodynamic mechanisms inside the cable-in-conduit conductor subsequent to the initiation of a propagating normal zone (during quench). This will allow design perturbation and optimization analysis and predict the failure mode (protection) behavior of large-scale MHD magnets. Although this work is progressing more slowly than expected, it continues to indicate the expected fail-safe operation.

The other path is to develop simple analytical solutions which bound the general design problem and enable the preliminary magnet design, which also parallels the conductor analytical effort. The following represents such a simplified analysis and shows good correlation with the experimental data.

1. Critical Current

As a check, we compare the manufacturer's number to the equations we are using for critical properties. For NbTi, the critical temperature is:

$$T_c(B) = T_{c0}(B)(1 - \frac{B}{B_{c20}})^{0.59}$$

where B_{c20} = 15 T, and T_{c0}(B) is 9.3 K. The critical current density (A/m^2) is given by

Miller in the ITER guidelines [MI89A], following Lubell's method [LU83]:

$$J_c(B,T) = J_{c)}\left[1 - \frac{t}{T_c(b)}\right]$$

where

$$J_{c0}(B) - J_{c00}\left(1 - \frac{b}{B_{c20}}\right)$$

and J_{c00} = 7300 A/mm^2. The calculated values of T_c and I_c are shown in Table II. The calculated values of T_c are sometimes a little higher, sometimes a little lower than the manufacturer's numbers. The calculated values of I_c are systematically about 10% higher than Supercon's. This implies that it might be acceptable to use 90% of the calculated values at fields other than 5, 6, and 7 T.

2. Power and Energy Balance

As a first approximation, the enthalpy available for recovery should be comparable to the enthalpy difference of helium between the bath and current sharing temperatures at constant mass density, when the conductor is in the well-cooled regime. The initial condition of the helium is believed to be 1 atm, 4.2 K, a mass density of 125 kg/m^3 and an enthalpy of 9.71 kJ/kg. However, our version of the NBS Helium Properties code returns 9.986 kg/kJ at 4.2 K and a density of 125 kg/m^3. Since we have to use this code to obtain untabulated values, this approximate value will be accepted throughout as the base enthalpy for calculations for energy margin. A table of calculated enthalpy differences and energy margins is shown in Table III.

5 T

(4.2 K, 1 atm, 125 kg/m^3, 9.986 kJ/kg, T_c = 6.9 K, $A_{strands}$=12.3 mm^2)

f_c	T_{cs}	p_{cs}	h_{cs}	h_{cs}-h_b	ΔH_{he}	$EM_{sleeved}$	$EM_{unsleev}$
	(K)	(MPa)	(kJ/kg)	(kJ/kg)	(kJ/m^3)	(mJ/cc)	(mJ/cc)
0	6.90		24.92	14.934	1866.75	1,001.67	1,138.26
0.1	6.63		23.28	13.294	1661.75	891.67	1,013.26
0.2	6.36		21.65	11.664	1458	782.34	889.02
0.3	6.09		20.02	10.034	1254.25	673.01	764.79
0.4	5.82		18.41	8.424	1053	565.02	642.07
0.5	5.55		16.81	6.824	853	457.71	520.12
0.6	5.28		15.22	5.234	654.25	351.06	398.93
0.7	5.01		14.23	4.244	530.5	284.66	323.48
0.8	4.74		12.82	2.834	354.25	190.09	216.01
0.9	4.47		11.41	1.424	178	95.51	108.54

6 T

(4.2 K, 1 atm, 125 kg/m^3, 9.986 kJ/kg, T_c = 6.5 K, $A_{strands}$=12.3 mm^2)

f_c	T_{cs}	p_{cs}	h_{cs}	h_{cs}-h_b	ΔH_{he}	$EM_{sleeved}$	$EM_{unsleev}$
	(K)	(MPa)	(kJ/kg)	(kJ/kg)	(kJ/m^3)	(mJ/cc)	(mJ/cc)
0	6.50		22.49	12.504	1563	838.68	953.05
0.1	6.27		21.1	11.114	1389.25	745.45	847.10
0.2	6.04		19.73	9.744	1218	653.56	742.68
0.3	5.81		18.35	8.364	1045.5	561.00	637.50
0.4	5.58		16.99	7.004	875.5	469.78	533.84
0.5	5.35		15.63	5.644	705.5	378.56	430.18
0.6	5.12		14.8	4.814	601.75	322.89	366.92
0.7	4.89		13.61	3.624	453	243.07	276.22
0.8	4.66		12.4	2.414	301.75	161.91	183.99
0.9	4.43		11.19	1.204	150.5	80.76	91.77

7 T

(4.2 K, 1 atm, 125 kg/m^3, 9.986 kJ/kg, T_c = 6.5 K)

f_c	T_{cs}	p	h_{cs}	h_{cs}-h_b	ΔH_{he}	$EM_{sleeved}$	$EM_{unsleev}$
	(K)	(MPa)	(kJ/kg)	(kJ/kg)	(kJ/m^3)	(mJ/cc)	(mJ/cc)
0	6.10		20.08	10.094	1261.75	677.04	769.36
0.1	5.91		18.95	8.964	1120.5	601.24	683.23
0.2	5.72		17.82	7.834	979.25	525.45	597.10
0.3	5.53		16.69	6.704	838	449.66	510.98
0.4	5.34		15.57	5.584	698	374.54	425.61
0.5	5.15		14.95	4.964	620.5	332.95	378.35
0.6	4.96		13.97	3.984	498	267.22	303.66
0.7	4.77		12.98	2.994	374.25	200.82	228.20
0.8	4.58		11.98	1.994	249.25	133.74	151.98
0.9	4.39		10.98	0.994	124.25	66.67	75.76

These approximate values for the energy margin in the well-cooled regime may be compared with the values measured in the experiments [MA89].

5 T Sleeved

I_{op}	f_c	Energy Dep	Quench
(kA)		(mJ/cc)	1=Yes
2.026	0.20	781	1
2.031	0.20	598	0
3	0.30	598	0
3.02	0.30	705	1
3.987	0.40	500	0
4.037	0.40	598	1
5.007	0.50	439	0

6 T Sleeved

I_{op}	f_c	EM	Quench
(kA)		(mJ/cc)	1=Yes
1.978	0.244197531	439	0
2.011	0.248271605	500	0
2.026	0.25	598	1
2.96	0.37	439	0
3.032	0.37	500	1
3.98	0.49	439	0
3.99	0.49	500	1
4.502	0.56	500	1
4.521	0.56	439	0
4.724	0.58	500	0
4.735	0.58	564	1
4.736	0.58	439	0

7 T Sleeved

I_{op} (kA)	f_c	Energy Dep (mJ/cc)	Quench Yes=1
2.01	0.3101852	705	1
2.021	0.31	598	1
2.011	0.31	439	1
2.053	0.32	195	0
2.044	0.32	305	0
2.049	0.32	356	1
2.991	0.46	195	0
2.994	0.46	305	0
3	0.46	356	1
3.5	0.54	195	0
3.48	0.54	305	0
3.49	0.54	356	1
4.002	0.62	305	0
4.002	0.62	356	1

7 T Unsleeved

I_{op} (kA)	f_c	Energy Dep (mJ/cc)	Quench Yes=1
2.015	0.31	3123	1
2	0.31	781	1
2.051	0.32	195	0
2.057	0.32	439	0
2.08	0.32	598	0
2.091	0.32	705	1
3.034	0.47	195	0
3.037	0.47	439	0
3	0.46	598	1
2.963	0.46	598	1
3.465	0.53	439	1
3.512	0.54	305	0

To simplify, take the average of the lowest quench energy and the highest nonquench energy at each field and current, and compare them with the available energy margin of the helium.

B (T)	f_c	EM_{exp} (mJ/cc)	Range (mJ/cc)	$EM_{He,avail}$ (mJ/cc)
5	0.2	689.5	183	782.3
5	0.3	651.5	107	673
5	0.4	549	98	565
6	0.25	549	98	607.28
6	0.37	469.5	61	497.146
6	0.49	469.5	61	387.682
6	0.56	469.5	61	345.158
6	0.58	532	64	334.024
7	0.315	372	134	438.392
7	0.46	330.5	51	349.586
7	0.54	330.5	51	306.658
7	0.62	330.5	51	253.94
Unsleeved				
7	0.315	689.5	183	498.1745
7	0.465	518.5	159	394.891
7	0.535	372	134	352.2085

The difference between the measured values of energy margin and the available enthalpy in the helium from the bath to the current-sharing temperatures are illustrated in the four

figures below. When the range between the minimum quenched case and the maximum recovery case is considered, the provable discrepancies, already small-looking, become even smaller.

CONCLUSION

For the most part, the discrepancies between the measured values of energy margin and the calculated enthalpy available in the helium between bath and current-sharing temperatures is not very large. Some of the disagreements cannot be explained qualitatively by simply looking at the available enthalpy. These include the rise in energy margin at the highest current point at 6 T and the flatness of the energy margin with fraction of critical current at 6 T and 7 T with an insulating sleeve. However, given the strong agreement between the crudest possible estimate of energy margin and the actually measured results over a broad range of discharges, we question whether further investigation of anomalous, "weird" results is justified. We suggest that we should proceed directly to attempt dynamic simulations of quench propagation.

The close agreement between measured energy margin and available helium enthalpy also suggests that helium enthalpy in the local heated region is the dominant source of stability, and that the following phenomena are secondary:

(1) The enthalpy of the copper, superconductor, conduit, and insulation.

(2) Axial heat leakage out of the heated region.

(3) Deposition of energy directly from the conduit to the cable in the uninsulated case, making power balance a factor at higher f_x.

5 T, Sleeved

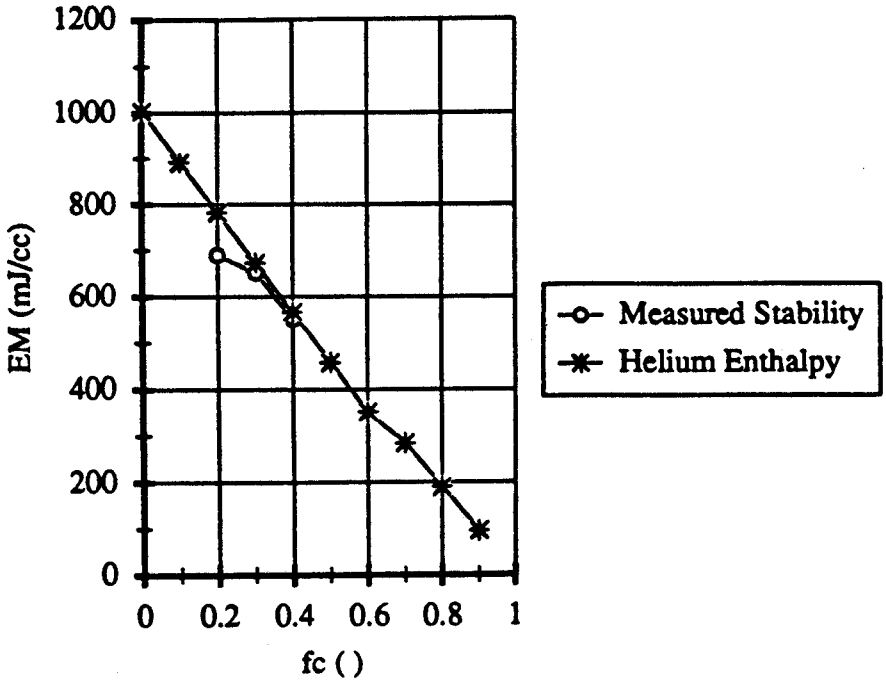

6 T. Sleeved

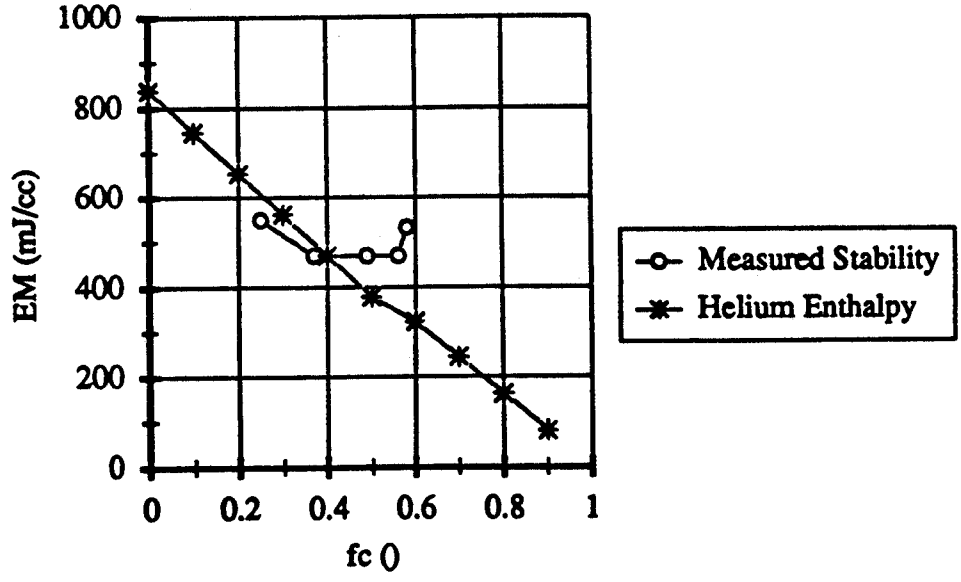

Figure 1 – Measured Stability and Helium Enthalpy - Sleeved Conductors

7 T, Sleeved

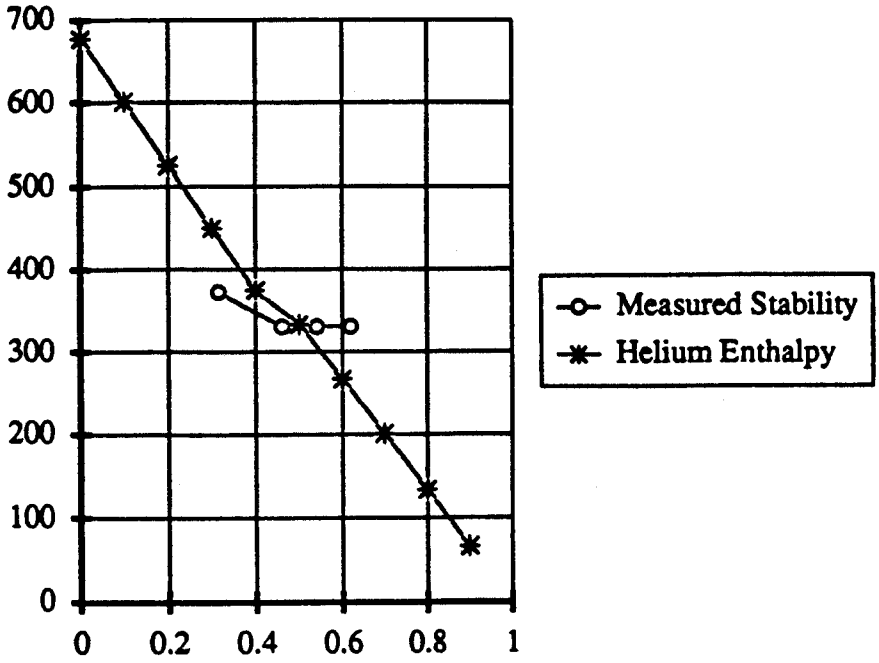

7 T, Unsleeved

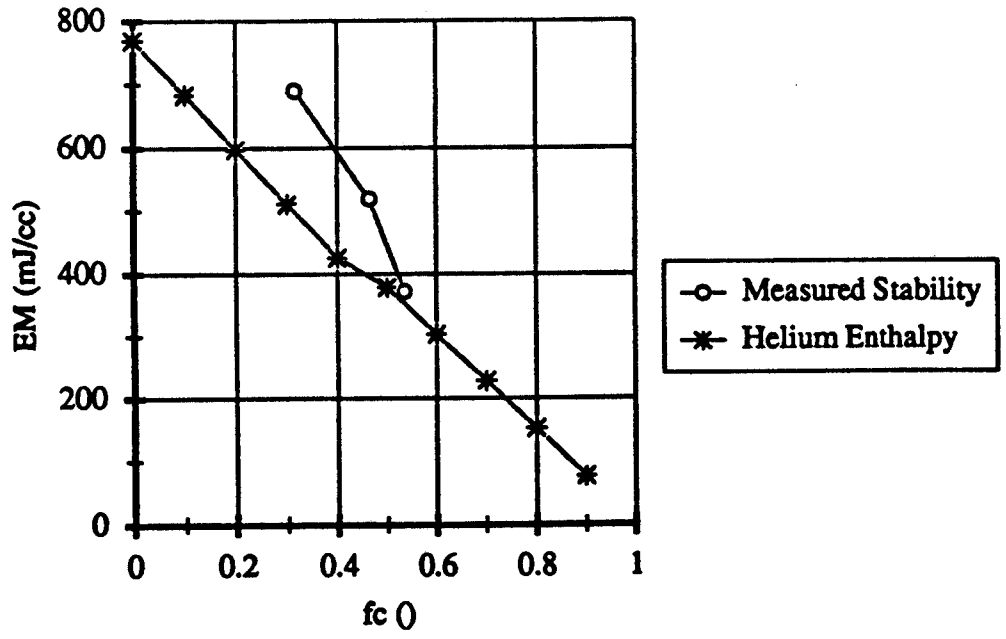

Figure 2 – Measured Stability and Helium Enthalpy - Unsleeved Conductors